*Materials Science-Poland, Vol. 24, No. 2/2, 2006*

# Nanogel formation by intrachain radiation-induced cross-linking. Simulation and experiment

P. ULAŃSKI[1], S. KADŁUBOWSKI[1], J. K. JESZKA[2, 3*]

[1]Institute of Applied Radiation Chemistry, Technical University of Łódź, ul. Wróblewskiego 15, 93-590 Łódź, Poland

[2]Centre of Molecular and Macromolecular Studies, Polish Academy of Sciences, ul. Sienkiewicza 112, 90-363 Łódź, Poland

[3]Department of Molecular Physics, Technical University of Łódź, ul. Żwirki 36, 90-924 Łódź, Poland

Nanogel formation by intrachain radiation-induced cross-linking is described. The origin of dispersive kinetics observed in pulse radiolysis experiments and the influence of cross-linking method on nanogel structure are studied by the Monte-Carlo simulation. The simulations have been performed on an *fcc* lattice using the cooperative motion algorithm. The recombination kinetics is studied as a function of the chain length (20–1068 beads) and of the number of radicals generated per chain. It is shown that the radical recombination rate coefficients are time-dependent (dispersive kinetics) and the simulation results can be fitted using single "stretched exponential" (KWW) function for two radicals per chain and a sum of two KWW functions for a larger number of radicals. The nanogel structure (radius of gyration and loop lengths, related to the resistance of nanogels to scissions) has also been studied. It is found that in the case of instant radical generation, the increasing number of radicals leads to formation of smaller and smaller loops. Results of the simulations are compared with the pulse radiolysis experiment on poly(ethylene oxide) using a suitable scaling of MC time and unit length, and a good agreement is obtained.

Key words*: Monte-Carlo simulations; polymer chain dynamics; cross-linking; radical recombination; nanogel; microgel; ionizing radiation*

## 1. Introduction

Nanogels are sub-micron-size water-swollen particles composed of three-dimensional network of hydrophilic polymer chains linked by permanent, covalent bonds. Since their size and shape resemble single linear macromolecules in a coiled conformation, nanogels can be regarded as internally cross-linked individual polymer chains. This combination of structure and size makes them unique and interesting for polymer

*Corresponding author, e-mail: jkjeszka@cbmm.lodz.pl

physicists and chemists, and allows them to be incorporated as a new item in the usual classification of polymer architectures, besides branched, star-like, dendritic etc. macromolecules. Nanogels, along with their larger analogues – microgels – have a broad range of actual and prospective applications. The most promising seem to be the applications in medicine and pharmacy, e.g. as polymeric drugs, stimuli-sensitive drug-delivery systems, cell markers and vectors [1, 2].

The most common way to synthesize nanogels and microgels is polymerization with cross-linking agents, usually in emulsion or microemulsion. Nanogels may also be obtained by the chemical intrachain cross-linking within single macromolecules [3]. Some time ago we have proposed an alternative method, based on intramolecular cross-linking induced by ionizing radiation [4]. In this method, a dilute aqueous solution of a polymer, free of any additives, is exposed to a high-dose pulse of fast electrons from an accelerator. As a result, several tens or even over a hundred radicals are generated almost instantaneously (typically within a microsecond) on each polymer chain. Since the distance between the chains is relatively high and their mutual diffusion is slow, most of the generated radicals undergo recombination with their neighbours within the same macromolecule. This method has been tested on a number of hydrophilic polymers [5–7].

In parallel to the synthetic aspects of this technique, we have studied the mechanism and kinetics of intramolecular recombination of polymer-derived mid-chain radicals [8, 9]. It has been found that the decay of radicals in these processes does not follow a classical, homogeneous second-order kinetics, typical of intermolecular recombination of radical pairs. When analyzed in these classical terms, the rate constant of intrachain recombination $k$ decreases in the course of reaction. This indicates that we deal with a dispersion of reactivity, and the dispersion changes in time. Therefore, we found it more appropriate to describe the intramolecular recombination by dispersive kinetics models, e.g. the one developed by Plonka [10].

$$k(t) = Bt^{a-1}, \qquad \frac{c_{(t)}}{c_0} = \exp\left(-Bt^{\alpha}/\alpha\right) \tag{1}$$

In fact, this model allowed us to obtain much better fits to experimental data, and parameter $\alpha$ could be very useful in assessing the width of the reactivity distribution. Nevertheless, application of the model still did not allow us to answer two important questions: (i) what is the main physical parameter governing the overall rate of intramolecular recombination, and (ii) what is the main origin of the non-classical kinetics, i.e. of the reactivity changes in time.

The objective of the current work is to perform more detailed studies of nanogel formation employing Monte Carlo simulations: to understand how the cross-linking proceeds, in particular what is the reason of the dispersive kinetics. This information can be used as a guideline, indicating how one can optimize the process of synthesis to obtain the best materials with predetermined properties.

In experiments one has to deal simultaneously with too many distributions (chain length, number of radicals generated per chain, distances between the radicals). It is

also impossible to exclude side reactions such as interchain recombination, radical transfer or chain scission. The ratio between the yields of recombination and the parallel reaction of disproportionation is set by chemical properties of the system and cannot be easily influenced. There are also technical and physical limitations: for instance one must use appropriate polymer concentrations and pulse intensities to get a sufficiently strong signal. One cannot therefore measure precisely enough small numbers of radicals per chain in very dilute solutions, especially in the final stages of the recombination process. The simulations give us a possibility to analyze the influence of various factors, eliminating the interference of others.

## 2. Pulse radiolysis studies on radical recombination

For experimental studies on the kinetics of intramolecular radical recombination we decided to use poly(ethylene oxide) (PEO) since, in contrast to most other simple water-soluble polymers, irradiation of this compound leads to the formation of only one kind of radicals. This allows to avoid potential problems that may result from a too complex reaction mechanism when many different radicals (of different absorption spectra, reactivity etc.) are present in the system.

Polymer standards of PEO (Polymer Laboratories, $M_p$ = 94 kDa and $M_p$ = 276 kDa, $M_w/M_n < 1.1$) were used to assure well defined chain length of relatively narrow distribution. We used 0.044 wt. % aqueous solutions of PEO (10 mM of monomer units), well below critical concentrations for coil overlap which were estimated as 0.26% and 0.15% respectively. The solutions were saturated with $N_2O$ to remove oxygen and to double the radiation-chemical yield of hydroxyl radicals, and then pulse-irradiated in quartz cells with 6 MeV electrons from a linear accelerator (electron path 7 mm, transverse optical path 10 mm). Electron pulses were of 0.5 μs duration and the dose per pulse could be varied from 100 to 400 Gy. Hydroxyl radicals resulting from the radiolysis of water reacted with PEO by hydrogen abstraction, generating mid-chain PEO radicals [11]. This reaction was essentially complete within the duration of the pulse. The decay of PEO radicals was followed by fast spectrophotometry at $\lambda$ = 270 nm. In order to obtain a reasonable signal-to-noise ratio, each recorded kinetic trace was an average of at least 16 individual shots. In calculations, the molar absorbance of PEO radicals at $\lambda$ = 270 nm has been assumed equal to 570 $dm^3 \cdot mol^{-1} \cdot cm^{-1}$, based on data from Ref. [11], and a small correction has been applied to compensate for a (very low) absorbance of stable final irradiation products.

## 3. Monte Carlo simulations

The nanogel formation process was simulated using the Monte-Carlo (MC) method on an *fcc* lattice, where the bonds have the same length. The possible bond angles are equal to 60, 90, 120 and 180° with the degeneracy 4, 2, 4 and 1, respec-

tively. Macromolecules are represented by ensembles of beads located on lattice sites, connected by non-breakable bonds. The number of beads in these simulations varied form 20 to over 1000, although most of the simulations were performed on 160 and 320 chains for which we can have sufficient statistics in a reasonable time. Movements of the polymer chains were simulated using the cooperative motion algorithm (CMA) [12–14], as a series of random displacements of segments on the lattice, observing integrity of the chains. MC time unit correspond to one attempt-to-move per bead. Radicals were simulated by ascribing to a bead the property of being able to form an additional bond with another "radical". If the distance between them was equal to the bond length, they could "react" (with some probability), i.e. they could form a bond (recombination and cross-linking) or disappear (the bead is no longer a "radical" – disproportionation). Thus the reaction rate was controlled by the chain dynamics. In each simulation cycle, one chain in a random conformation, with $Z_0$ radicals on it, was generated and surrounding beads imitated a good solvent. Thus the interchain recombination was not possible.

Fig. 1. Screenshot of a chain $N = 1280$ with $Z_0 = 16$ radicals during simulations. Grey circles mark radicals which have not recombined yet and black circles are the beads on which a radical has recombined forming cross-linking bonds and loops

Decay kinetics were averaged over at least 400 radical pairs (except for some simulation for very long chains and long times). We analysed time evolutions of the average number of radicals, length of loops, radius of gyration, and end-to-end and bond vector **R** autocorrelation functions

$$\rho_{(t)} = \frac{1}{n}\sum_{i=1}^{n} R_{i(0)} R_{i(t)} \tag{2}$$

In the above equation, $R_{i(0)}$ denotes the **R** vector of a chain (or a bond) $i$ at the beginning of the simulation ($t = 0$) and $R_{i(t)}$ the vector at a time $t$. By fitting $\rho(t)$ to so -called stretched exponential (Kohlrausch–Williams–Watts) function

$$\rho_{(t)} = \exp\left[-\left(\frac{t}{\tau}\right)^{\beta}\right] \tag{3}$$

we can determine the relaxation time $\tau$ and dispersion parameter $\beta$. This function is equivalent to the first order dispersive kinetics and was also used in the analysis of radical decays.

The loop length is defined as the number of bonds between the radicals that recombined. Thus in the case of Z > 2 the same bead may belong to more than one loop. The total loop length $L$ is a sum of lengths of successively formed $(Z_0 - Z)/2$ loops. Figure 1 shows a snapshot of a chain on which a part of the radicals recombined.

## 4. Results and discussion

Experiments and simulations show that the factors influencing the radical decay kinetics are the initial number of radicals per chain, and the chain length. This is illustrated in Figure 2 showing the evolution of average number of radicals in the simulations in which four radicals are generated at random on chains of different length, and in Figure 3 showing normalised radical decays on chains of different length if the ratio of chain length $N$ to the number of initially generated radicals $Z_0$ is constant.

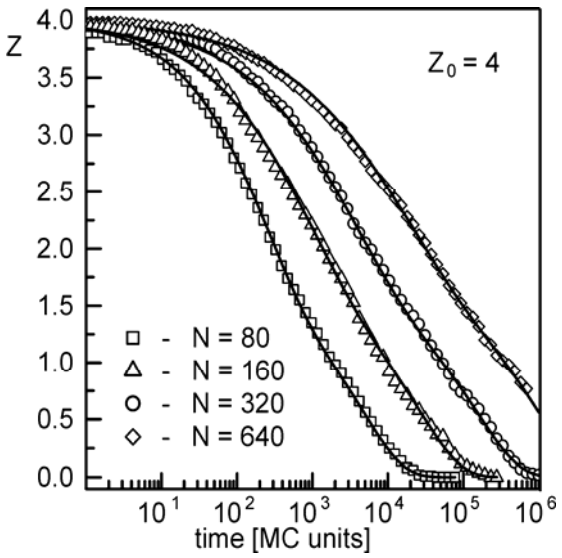


Fig. 2. Radical decay kinetics for four radicals generated on chains of different lengths. Solid lines show fits using sums of two stretched exponential functions (Eq. (4)); $C$ = 0.65 in all cases

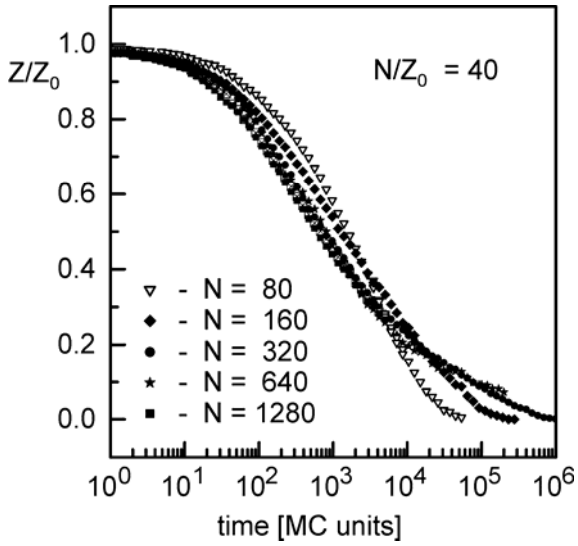


Fig. 3. Radical decay on chains of different lengths when the initial radical density on the chain $N/Z_0 = 40$

In Figure 2, one can see that the radical recombination strongly depends on the chain length, the radical decay half time $t_{1/2}$ being proportional to $N^{2.3}$. Similar dependences were found for other numbers of radicals. However, in the simulations presented in Figure 2, both the chain length and average distance between the radicals (measured along the chain contour) increase. It is therefore not clear which factor dominates. The results shown in Figure 3 clearly demonstrate, however, that the average distance is the most important parameter controlling the decay rate. It can be seen that if the ratio $N/Z_0$ (related to the average distance between the radicals), is constant, then the decay half time is only slightly dependent on $N$. At short times (shorter than ca. $5t^{1/2}$) the time dependence is practically independent of the chain length for longer chains. However, it changes qualitatively at longer times where the effect of chain length becomes very important. This result can be explained taking into account that at first radicals recombine mostly with the nearest neighbours hence this process is weakly dependent on the chain length if $N/Z_0$ is constant. By contrast, at the last stage the average distance between the remaining radicals is the larger the longer is the chain, thus the recombination kinetics becomes strongly dependent on the chain length. The process cannot therefore be adequately described by a single kinetic equation.

The decay kinetics was found to be practically identical in simulations in which no cross-linking took place (disproportionation), although one could expect formation of loops to give rise to sterical obstacles making recombination slower. This effect will be addressed in more detail in a forthcoming paper [15].

Results of simulations for $Z_0 = 2$ can be fitted using a single stretched exponential function (Eq. (4)) but for $Z_0 > 2$ a sum of at least two stretched exponentials must be used to achieve satisfactory fits (shown as lines in Fig. 2).

$$\frac{Z}{Z_0} = C\exp\left[-\left(\frac{t}{\tau_1}\right)^{\beta_1}\right] + (1-C)\exp\left[-\left(\frac{t}{\tau_2}\right)^{\beta_2}\right] \tag{4}$$

Systematic simulations for constant $Z$ and variable $N$ make possible determination of trends in $N$ or $Z_0$ dependences of the parameters $\tau$, $\beta$ and $C$, and interpolations/extrapolations [15] allowing comparison with the experiments using high molecular weight polymers for which a direct simulation would be extremely time-consuming. Evolution of other parameters which change during the radical recombination is presented in Figure 4.

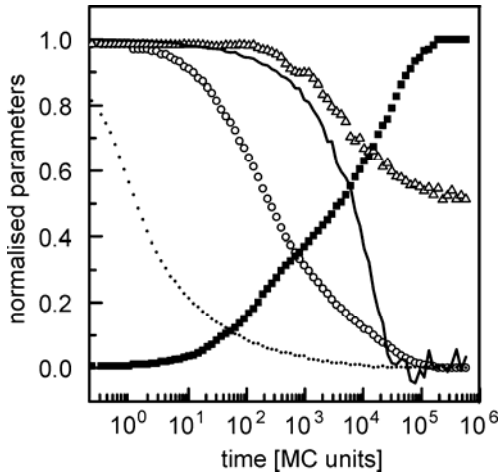


Fig. 4. Time dependences of normalised parameters of the nanogel during recombination of eight radicals ($N$ = 160). Circles – radical number $Z/Z_0$, filled squares – total loop length $L/L_f$, triangles – radius of gyration $R_g^2/R_{g0}^2$. The solid line shows the decay of the end-to-end ($\rho_{EE}$) and the dotted line – bond ($\rho_B$) autocorrelation functions

One can see that the average total loop length $L$ (related to the resistance of nanogels to chain scissions) increases during the cross-linking process and attains its final value $L_f$ when all the radicals have recombined. This increase is, however, slower than the radical decay (the total loop length attains half of its final value at a time ca. ten times longer than the radical decay half-time). The decrease of the radius of gyration $R_g$ due to cross-linking is even slower than the increase of loop length, which can be explained taking into account that attaining equilibrium $R_g$ needs some additional time of the order of the end-to-end vector relaxation time to reach equilibrium chain conformation after the cross-linking event.

Simulations carried out for different $Z_0$ show that $L_f$ increases sub-linearly with increasing number of generated radicals ($L_f \sim Z_0^{0.5}$). This effect is related to the fact that when $Z_0$ increases, the average distance between the radicals decreases, hence shorter

and shorter loops are formed. Based on these simulations, we can predict that this limitation can be suppressed by generation of a smaller number of radicals in suitable time intervals, e.g. using sequences of short pulses. This effect, however, has not yet been confirmed experimentally.

## 5. Comparison with experiment

Figure 5 presents a comparison of experimental results obtained on monodisperse samples of molecular weight 94 and 276 kDa (2140 and 6290 monomer units). One can see that these results are in a qualitative agreement with the simulations: if the average concentrations of radicals on a chain are the same, the decay half times are very similar and the experimental time dependence corresponds well to simulations of multiple randomly distributed radicals on long chains. The obtained results can be directly compared with the simulations performed assuming that two monomer units correspond to one MC segment, and an MC time unit is taken equal to $5\times10^{-9}$ s (small symbols). Such a time scaling is justified not only by the correspondence of the experimental and simulation results but also by a correspondence of the orientation relaxation times. From the simulations we can also obtain the relaxation time of an MC

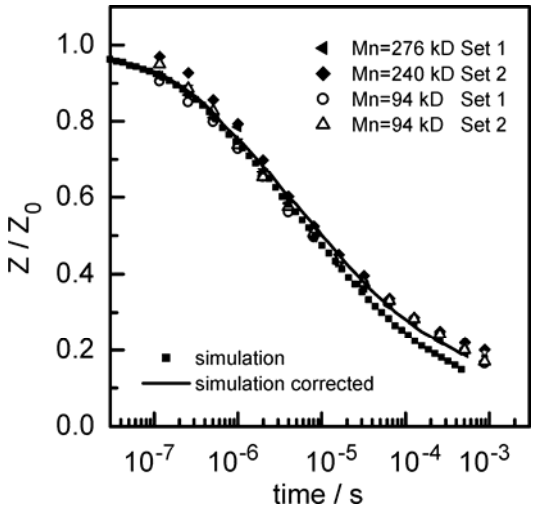


Fig. 5. A comparison of experimental and simulated radical decays. In the experiment, $N_2O$-saturated aqueous 10 mM PEO solutions were pulse-irradiated with an average dose of 330 Gy per pulse. Full symbols: $M_p$ = 276 kDa ($<Z_0> \cong 60$), empty symbols: $M_p$ = 94 kDa ($<Z_0> \cong 20$), diamonds: simulation for $N$ = 1068, $Z_0$ = 20. The solid line shows simulation results corrected for odd numbers of radicals. The Monte Carlo scaling method is described in the text

segment equal to 2 MC time units. The relaxation time for the Kuhn segment of PEO (6 atomic bonds) in water, determined by molecular dynamics simulations, is ca. $3\times10^{-10}$ s

[16]. Thus taking into account that only some contacts between beads in the simulations correspond to configuration for which the radicals can recombine, we can conclude that such a time scaling is reasonable. Some additional correction should be made taking into account that in the simulations an even number of radicals per chain was assumed. In a real system we generate odd and even number of radicals thus some of the radicals cannot recombine by intrachain recombination mechanism. The result of simulations corrected for this factor is shown in Fig. 5 as a solid line. One can see that the results of simulations and experiment are in a good agreement confirming that the intrachain radical recombination is governed by chain dynamics.

## 6. Conclusions

A good agreement between of the results of pulse radiolysis experiments and MC simulations of the chain dynamics-controlled radical recombination indicate that the assumed simulation model can be used to gain insight into behaviour of real systems. Simulations of intrachain cross-linking provide information on the role of different parameters and phenomena in nanogel formation. Because of the strong dependence of the recombination rate on the distance between the radicals ($t_{1/2} \sim R^{2.3}$), the recombination of nearest neighbours is strongly favoured. In the case of a statistical generation of radicals, the average distance between nearest neighbour radicals is the most important factor controlling the reaction rate constant. Distribution of nearest-neighbour distances seems to be the main reason of dispersive kinetics.

The simulations provide also an information on the effect of various parameters on the structure of the nanogel, strongly related to the kinetics of the process. If the number of generated radicals is increased, mostly shorter, less efficient loops are formed. It can be predicted how the nanogel structure and related properties can be controlled by a modification of the radical generation procedure.

**Acknowledgements**

The authors thank Professor Tadeusz Pakula (Max-Planck Institute for Polymer Research, Mainz, Germany) for making available the basic code of chain motion and valuable discussions, and the LINAC staff headed by dr. Krzysztof Hodyr (TU Lodz) for their valuable technical assistance. This work has been supported in part by the International Atomic Energy Agency (TCP POL/6/007) and NATO (PST.MEM.CLG 980622).

## References

[1] FUNKE W., OKAY O., JOOS-MÜLLER B., Adv. Polym. Sci., 136 (1998), 139.
[2] ULANSKI P., ROSIAK J.M., *Polymeric Nano- and Microgels*, [in:] H.S. Nalwa (Ed.), *Encyclopedia of Nanoscience and Nanotechnology*, American Scientific Publishers, Stevenson Ranch, CA, 2004, Vol. 8, p. 845.
[3] BRASCH U., BURCHARD W., Macromol. Chem. Phys., 197 (1996), 223.
[4] ULANSKI P., JANIK I., ROSIAK J.M., Radiat. Phys. Chem., 52 (1998), 289.

[5] ULANSKI P., ROSIAK J.M., Nucl. Instr. Meth., B 151 (1999), 356.
[6] KADLUBOWSKI S., GROBELNY J., OLEJNICZAK W., CICHOMSKI M., ULANSKI P., Macromolecules, 36 (2003), 2484.
[7] ARNDT K.-F., SCHMIDT T., REICHELT R., Polymer, 42 (2001), 6785.
[8] ULANSKI P., ZAINUDDIN, ROSIAK J.M., Radiat. Phys. Chem., 46 (1995), 917.
[9] ULANSKI P., KADLUBOWSKI S., ROSIAK J.M., Radiat. Phys. Chem., 63 (2002), 533.
[10] PLONKA A., *Dispersive Kinetics*, Kluwer Acad. Publ., Dordrecht, 2001.
[11] ULANSKI P., ZAINUDDIN, ROSIAK J.M., Radiat. Phys. Chem., 46 (1995), 913.
[12] PAKULA T., Macromolecules, 20 (1987), 679.
[13] PAKULA T., GEYLER S., Macromolecules, 20 (1987), 2909.
[14] PAKULA T., JESZKA K., Macromolecules, 32 (1999), 6821.
[15] JESZKA J.K., KADLUBOWSKI S., ULANSKI P., Macromolecules, 39 (2006), 857.
[16] BORODIN O., BEDROV D., SMITH G.D., Macromolecules, 34 (2001), 5687.

*Received 29 April 2005*
*Revised 30 November 2005*